Dynamics of the guest-host orientational interaction in dye-doped liquid-crystalline materials

Thai V. Truong, Lei Xu,* and Y. R. Shen†
Department of Physics, University of California, Berkeley, California 94720, USA
(Received 16 June 2005; published 14 November 2005)

We present a comprehensive study on the dynamics of laser-induced molecular reorientation in a dye-doped liquid crystalline (LC) medium that exhibits significant enhancement of the optical Kerr nonlinearity due to guest-host interaction. Using various techniques, we separately characterized the dynamical responses of the relevant molecular species present in the medium following photoexcitation and, thus, were able to follow the transient process in which photoexcitation of the dye molecules exert through guest-host interaction a net torque on the host LC material, leading to the observed enhanced optical Kerr nonlinearity. Experimental results agree quantitatively with the time-dependent theory based on a mean-field model of the guest-host interaction.

DOI: 10.1103/PhysRevE.72.051709 PACS number(s): 61.30.−v, 42.70.Df, 78.47.+p, 42.65.−k

I. INTRODUCTION

It has been long appreciated in a wide number of fields how a small amount of guest substance could interact with a host material and drastically change the properties of the host material. This guest-host interaction has been exploited in designing new materials with desirable properties which are not present in the pure host materials. In the field of liquid crystals (LC), due to the correlated nature of LCs, often the effect of impurities is greatly amplified. Guest-host interactions have long been used to both modify the properties and gain understanding of the LC host materials. Examples include impurity-induced changes of phase transition temperatures, optical Kerr nonlinearity, photorefractivity, and modification of chiral structures of LCs [1–4].

Beside the already huge role that LCs play in the display industry, in the last decade or so there has been a push to take advantage of the large optical Kerr nonlinearity of LCs in a wide variety of device applications in the optoelectronics industry [4–6]. The large optical Kerr nonlinearity of LCs comes from their highly anisotropic molecular structures, making them readily reoriented by an optical field [5,6]. In 1990, Jánossy discovered that the optical reorientation of nematic LCs can be enhanced up to two orders of magnitude upon doping with certain absorbing dichroic dyes when the dye molecules are excited anistropically [7]. Phenomenologically, the enhanced reorientation could be described by an extra torque that is proportional to the optical torque, though the elastic constants of the dye-doped materials remain practically the same as the pure materials. Subsequent experimental works [8–10] showed that the enhanced optical reorientation could not be explained by usual mechanisms following dye excitation such as thermal effects and photoisomerization of the dye as in the case with the azo dye [11]. The enhanced reorientation could have either a positive or negative sign, i.e., the extra torque resulting from dye excitation could reorient the host molecules either parallel or perpendicular to the linearly polarized light field [10,12,13]. While the effect relies on optical excitation of the dye, earlier studies on pump-wavelength dependence found that the extra torque did not simply follow the absorption band profile [14,15]. A recent study, however, did find the simple wavelength dependence [16]. Investigation of how the effect depends on the molecular structures of the guest and host showed that it is sensitive to the structural change and isotopic substitution of the substituent groups in the dye molecule, pointing to the importance of dipolar interactions between guest and host molecules [17–19]. The enhanced optical reorientation due to dye-doping, known as the Jánossy effect, was also found to be not limited to nematic LCs, but also present in isotropic liquids [20–22]. Thus, the effect is quite general.

Jánossy has proposed a mean-field model to explain the effect [23], which is based on two main processes. First, optical excitation of the dichroic dye yields an oriented population in the excited state and an oriented hole in the ground-state population. Then, the dye molecules in the excited and the ground states exert different reorienting torques on the host molecules through their respective molecular orientational couplings with the host, resulting in a net torque on the host molecules and, hence, the enhanced reorientation. In Jánossy's model, the guest-host interaction is described by a mean-field approximation. Marrucci *et al.* recognized that in addition to the anisotropic orientational coupling, the isotropic interaction between guest and host molecules, which is manifested in the rotational diffusion coefficients of the guest molecules, could also play a role in determining the extra reorienting torque [21,24].

The model described above has been consistent with the results found in earlier experimental studies [25,26]. The key assumption of the model is that upon photoinduced excitation of the guest molecules, the guest-host orientational interaction and the rotational diffusion of the guest change significantly. In a recent study [27], it was found that rotational diffusion of dye molecules in the ground and excited states are indeed very different. The extra torque on host molecules generated by the dye is inherently transient, lasting only

*Present address: Department of Optical Science and Engineering, Fudan University, China.
†Corresponding author. Email address: shenyr@socrates.berkeley.edu

when the anisotropic population of the dye excited and ground states are present. Nevertheless, only steady-state or quasi-steady-state behavior of the Jánossy effect was studied in the earlier studies. As is well known, comparing model predictions with experimental observations of the dynamic behavior of the guest-host system would certainly constitute a more stringent test of the model. One would like to measure the orientational dynamics of both guest and host molecules and, thus, be able to follow the transient reorienting torque the guest exerts on the host. One would like to learn from the early dynamics of the system whether the mean-field model for the guest-host interactions is still valid during the period when various molecular relaxations just begin to set in.

We recently reported our experimental study of the dynamics of the guest-host interactions of dye-doped LC in the isotropic phase [28,29], addressing the issues discussed above. In this paper, we provide the details of our study with some minor corrections to the results reported in Ref. [28]. We used various techniques to carry out a series of quasi-steady-state and time-resolved measurements of the optical Kerr responses of both pure and dye-doped LC systems to characterize separately the picosecond to nanosecond orientational dynamics of host molecules, excited-state guest molecules, and ground-state guest molecules. This allows us to follow the host response to the reorienting torque generated by the excitation of the guest molecules. A mean-field model of guest-host interaction was found to agree well with our experimental observation. From the transient study, we have gained further insights into the reorientation of the host by guest-host interaction that gives rise to the enhanced optical Kerr nonlinearity.

The Jánossy effect could be seen as a special case of the solvation process, a subject that is of wide interest [30]. In the past, solvation was often studied through observation on reporter chromophores that reflect the solvent effects on the reporter molecule. Only recently have there been studies that looked at the response of the solvent, which provides complementary information on solvation [31–33]. Seen in this light, our study can be considered a comprehensive study of the orientational solvation dynamics of a guest-host system.

The rest of the paper is organized as follows. In Sec. II, we describe the quantitative theoretical model, based on the physical picture described above, extended to the transient regime. In Sec. III, we present the series of experiments that were carried out to study the orientational dynamics of the guest-host system, followed by a discussion of the observed enhancement effect and a conclusion in Sec. IV.

II. THEORY

A. Physical model

We adopt here the model proposed by Jánossy [23] and extended by Marrucci *et al.* [21,24]. For simplicity, consider a guest-host system in the isotropic liquid phase consisting of the LC host and the dye guest, both of which have effective rod-like molecular structures. An incoming linearly polarized optical pump field has two effects on molecules that may directly create an anisotropic orientational distribution of molecules in the otherwise isotropic system. One is to reorient the molecules toward the field direction by the optical torque against thermal randomization. The other is to excite the molecules to an excited state, preferentially along the field direction. The latter process is generally much more effective in creating the anisotropy than the former and, therefore, if present, easily dominates over the former. In our study, the pump field excites only the dye molecules and not the LC molecules. Then concerning the direct action of the optical field, we need to consider only the polarized excitation of the dye molecules and the field-induced reorientation of the LC molecules.

The optical excitation of the dye molecules results in three different molecular species in the system: ground-state dye molecules, excited-state dye molecules, and host LC molecules, denoted by the subindices $i=g$, e, and h, respectively. The excited-state dye molecules have an orientational distribution peaked along the linear polarization of the pump field while the ground-state dye molecules have a corresponding hole in the orientational distribution. Both are influenced by orientational relaxation (due to rotational Brownian motion) and spontaneous de-excitation of the dye molecules. The anisotropic distributions of both the excited-state and the ground-state dye molecules can reorient the LC host molecules via guest-host intermolecular interactions. The former tries to align the LC molecules along the field, and the latter perpendicular to the field. We expect an enhanced reorientation effect on the LC host if the former action is stronger than the latter, but the opposite effect if the reverse is true.

A natural question arises on whether the guest-host interaction can be strong enough to yield significant enhancement of the optical-field-induced reorientation, considering that the concentration of the excited-state dye molecules is quite small. We provide here an order-of-magnitude comparison of the average reorientational potentials exerted on a LC molecule due to the direct optical torque and due to the guest-host interaction. Regarding the former, a light pulse of intensity I produces on a LC molecule a reorientational potential [34]: $V_{direct} \approx 2\pi\Delta\alpha' L^2 I/nc$, where $\Delta\alpha'$ is the polarizability anisotropy of the LC molecule; $L=(n^2+2)/3$ is the Lorenz-Lorentz local-field factor; n is the average refractive index; and c is the light speed in vacuum. For a typical LC molecule [35], $\Delta\alpha'=20$ Å^3 and $n=1.5$, we find $V_{direct}=3.5\times10^{-7}$ eV for $I=10^7$ W/cm^2 $=10^{14}$ erg/(s cm^2).

For the guest-host reorientational potential, consider the representative molecular structures of the dye guest and LC host in Fig. 1. Although the exact nature of the guest-host orientational interaction is still under question, we assume that dipole-dipole interaction between the amino group of the guest molecules and the nitrile group of the host molecules is the main mode of interaction. The orientational potential for such dipole groups is of the order 0.1 eV per nearest-neighbor pair in the liquid state [36]. If each guest molecule has two LC nearest neighbors, and the dipolar interaction beyond the nearest neighbor is negligible, then with the typical doping concentration of 1 guest for 1000 host molecules, we have, on average, an orientational potential per LC molecule due to an oriented guest molecule $U_{guest}=0.1$ eV $\times(2/1000)=2\times10^{-4}$ eV.

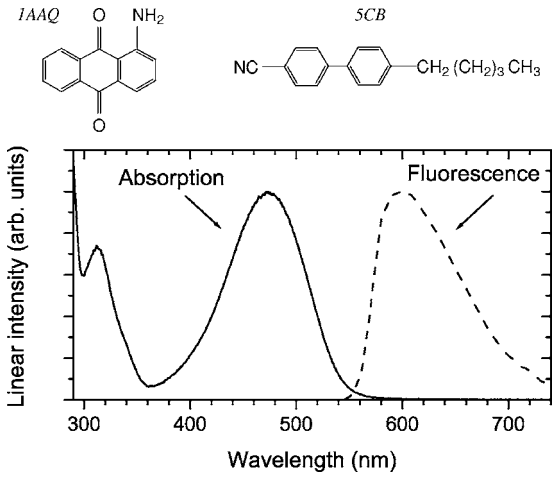

FIG. 1. Molecular structures of 1AAQ and 5CB and the absorption and fluorescence spectra of 1AAQ in 5CB. 5CB absorption has been subtracted out.

Now, the guest-host interactions are different for molecules in the ground and excited states. If 1% of the ground-state population is pumped into the excited state, and U_{guest} of the ground and excited states of dye differ by 10%, then the average guest-host reorientational potential exerted on a LC molecule is $V_{guest}=1\%\times 10\%\times U_{guest}=2\times 10^{-7}$ eV, comparable to V_{direct} estimated above. This shows that indeed guest-host interaction could be strong enough to significantly enhance the optical reorientation of LC molecules.

In the case of a pulsed laser excitation, the dye-induced LC reorientation mechanism is expected to decay away when the excited dye molecules return to the ground state and the anisotropy in the orientational distributions of the dye molecules diminishes toward thermal equilibrium. The dynamics of the dye molecules is then governed by the rotational diffusion equations under the simultaneous actions of optical excitation and spontaneous de-excitation. With a sufficiently short excitation pulse, the dynamics of dye relaxation basically evolves after the pulse is over. If the dye relaxation is much faster than the orientational relaxation of the LC molecules, then the reorienting effect of the dye guest on the LC host is essentially cumulative.

The above picture provides a qualitative description of the dye-induced enhancement effect on optical-field-induced reorientation of LC. Following this picture, we can now formulate the theory to provide a quantitative description of the effect.

B. Formalism of dynamic equations

The orientation of a rod-like molecule can be specified by a single angle θ formed by the long molecular axis and the field direction, and the time-dependent molecular orientational distribution for the i-type molecules is described by the distribution function $f_i(\theta,t)$, which can be expanded into a series of Legendre polynomials P_l as

$$f_i(\theta,t)=\frac{1}{4\pi}\sum_{l=0,2,4,\ldots}(2l+1)Q_i^{(l)}(t)P_l(\cos\theta), \tag{1}$$

where

$$Q_i^{(l)}(t)=\int f_i(\theta,t)P_l(\cos\theta)d\Omega \tag{2}$$

are the Legendre moments of the distribution. Note that all odd-l moments are zero due to the inversion symmetry of the system. Specifically, the zeroth-order moment $Q_i^{(0)}(t)=N_i(t)$ is the number density of the i-type molecular species and the second-order moments divided by the number densities, $Q_I^{(2)}(t)/N_i(t)$, are the usual orientational order parameters. In our study, we limit ourselves to the case of low optical pumping intensity, i.e., the induced orientational ordering is small, hence only $Q_i^{(2)}$ plays a role. We shall then simply write Q_i for $Q_i^{(2)}$. The rotational dynamics of the system is described by the three functions $Q_i(t)$ for the three molecular species. An alternative and equivalent way to define $Q_i(t)$ is by

$$Q_i=\langle S_i\rangle/V$$

$$\text{with } S_i=\sum_m s_i^m\equiv\sum_m\frac{1}{2}(3\cos^2\theta_i^m-1), \tag{3}$$

where the sum is over the total number of the i-type molecules under consideration; $\theta_{i,m}$ is the angle between the long axis of the molecule and the optical field; V is the volume of the sample; and the angular brackets denote the ensemble average. In an isotropic system, $f_i(\theta,t)$ has no θ dependence and $Q_i=0$.

The equations of motion for Q_i originate from the rotational Brownian motion of the molecular species. We consider here first the dye molecules in the ground and excited states, $i=g$ and e, respectively. In the limit where the rotational Brownian motion consists of small angular steps and can be approximated as a continuous diffusional process described by a rotational diffusion coefficient D_i, the distribution function $f_i(\theta,t)$ obeys the following Einstein-Schomulchowski equation:

$$\frac{\partial}{\partial t}f_i-D_i\frac{1}{\sin\theta}\frac{\partial}{\partial\theta}\sin\theta\left(\frac{\partial}{\partial\theta}\right)f_i=W_i. \tag{4}$$

Here, W_i with $i=g$ and e are the rates of transitions into the ground and excited states, respectively. They are given by

$$W_e(\theta,t)=+p(\theta)f_g(\theta,t)-\frac{f_e(\theta,t)}{\tau_f}, \tag{5}$$

$$W_g(\theta,t)=-p(\theta)f_g(\theta,t)+F\frac{f_e(\theta,t)}{\tau_f}+(1-F)\frac{K(t)}{\tau_f}, \tag{6}$$

where $p(\theta)=(3\beta I\cos^2\theta)/(h\nu N_d)$ is the pump excitation rate assuming that the transition dipole is parallel to the long molecular axis; ν and I are the optical pump frequency and intensity, respectively; β is the linear absorption coefficient; h is the Planck's constant; N_d is the total dye number density; and τ_f is the excited-state lifetime. The constant F denotes the fraction of molecules preserving their orientation when relaxing from the excited state to the ground state. $F=1$ means molecular orientation is the same before and after the relaxation, whereas $F=0$ means the decay process com-

pletely erases any orientational "memory" of the molecules. The $K(t)$ term in Eq. (6) describes the depopulation component that completely randomizes molecular orientation, with $K(t)=N_e(t)/4\pi$ obtained from the condition $\int W_e(\theta)d\Omega=-\int W_g(\theta)d\Omega$. For radiative transitions, F is expected to be 1. In the literature, based on physical argument, $F=1$ is also often assumed for nonradiative transitions, although it has never been experimentally verified, due to technical difficulties [29]. We leave F as a parameter in our dynamical equations, but will take the assumption of $F=1$ in later quantitative data analysis.

In Eqs. (5) and (6), we have neglected the optical torque on the dye molecules because its effect in generating orientational anisotropy in the dye population is much smaller than that of the polarized optical excitation. We have also neglected, in Eq. (4), interactions between dye molecules because of their low concentration and the effect of the light-induced LC anisotropy on dye molecules because at the relatively low pump intensity Q_h/N_h is very small ($\leqslant 10^{-5}$). The equations for Q_e and Q_g can be obtained readily from multiplying Eq. (4) by $P_2(\cos\theta)=\frac{1}{2}(3\cos^2\theta-1)$ and integrate over the solid angle. We find

$$\left(\frac{\partial}{\partial t}+\frac{1}{\tau_{De}}\right)Q_e=-\frac{1}{\tau_f}Q_e+AI(t),$$

$$\left(\frac{\partial}{\partial t}+\frac{1}{\tau_{Dg}}\right)Q_g=+\frac{F}{\tau_f}Q_e-AI(t), \tag{7}$$

where $\tau_{Di}\equiv 1/6D_i$ is the rotational diffusion time of the i-type species, and $A\equiv 2\beta/5h\nu$. The above equations are essentially the same as those of Marrucci *et al.* [21] in the low excitation intensity limit. The solutions of Eq. (7) for Q_e and Q_g are

$$Q_e(t)=\int_{-\infty}^{t}AI(t')e^{-(t-t')/\tau_{Qe}}dt',$$

$$Q_g(t)=\int_{-\infty}^{t}\left[\frac{F}{\tau_f}Q_e(t')-AI(t')\right]e^{-(t-t')/\tau_{Dg}}dt', \tag{8}$$

with $\tau_{Qe}\equiv(1/\tau_{De}+1/\tau_f)^{-1}$. Equations (8) completely describe the rotational dynamics of the dye molecules.

We now turn to the discussion of Q_h for the host LC molecules. In principle, a similar derivation starting from the rotational diffusion equation for the orientational distribution of the LC molecules influenced by the optical torque would yield the equation of motion for Q_h. However, the situation here is complicated by the characteristically strong orientational interactions between neighboring LC molecules. In fact, it is this strong intermolecular orientational coupling that gives rise the nematic phase of the LC as the temperature is lowered from the isotropic phase. For the sake of clarity, we first review the rotational dynamics of pure LC in the isotropic phase. This topic has received considerable interests, both theoretically and experimentally, over the last three decades [36–53]. Though a complete understanding of the subject seems still missing [50–53], many salient features have been understood.

The strong orientational coupling between LC molecules gives rise to local orientational orderings, which are usually visualized as microscopic pseudonematic domains existing in the macroscopically isotropic system [36,37]. Orientational fluctuation of these domains, or, equivalently, randomization of their directors with respect to each other after a reorienting torque, gives rise to the well-known collective response with exponential decay time in the range of nanoseconds and above. This collective response of LC is described well by the Landau-de Gennes theory treating the LC intermolecular interactions as a mean-field [36–41,45,46]. As the temperature is lowered toward the isotropic-nematic transition, the size of the pseudonematic domains, and thus the collective response decay time, tend to diverge, exhibiting characteristic pretransitional behavior. Beyond the mean-field approximation, or, equivalently, beyond orientational relaxation through randomization of the pseudonematic domains with respect to each other, the interactions between the neighboring molecules result in a number of other modes of relaxation with much shorter orientational relaxation times, reflecting molecular orientational behavior from within the pseudonematic domains down to individual molecules. These relaxation modes exhibit no pretransitional behavior and have been experimentally observed, both in the frequency domain [43] and time domain [44,48,50].

The description of LC rotational dynamics with multiple orientational relaxation times was formulated earlier by Flytzanis and Shen [42], where the intermolecular interaction between LC molecules are taken into account beyond the mean field by a perturbative calculation following Zwanzig's iterative approach [54]. This treatment, though at best is an approximation to the yet-to-be-found complete solution to the problem, is the only model available presently that provides an analytical expression for the LC rotational dynamics, and as will be shown later, explains our experimental data quite well. We briefly sketch their derivation here.

From Kubo's fluctuation-dissipation theory, the induced anisotropy due to an optical field of frequency Ω is given by

$$Q_h(\Omega)=\frac{2\Delta\alpha_h'}{3k_BTV}\left[\langle S_h(0)S_h(0)\rangle+i\Omega\int_0^\infty\langle S_h(0)S_h(t)\rangle e^{-i\Omega t}dt\right]\times|\mathcal{E}_{loc}|_\Omega^2\equiv\gamma(\Omega)|\mathcal{E}_{loc}|_\Omega^2. \tag{9}$$

Here, k_BT is the thermal energy and $\mathcal{E}_{loc}$ is the local field, which represents the overall reorienting field felt by an individual LC molecule. It is the sum of the applied field $\mathcal{E}_0$ and the mean-orienting field created by neighboring LC molecules. In terms of interaction energy, the total reorientational potential energy experienced by the mth LC molecule is

$$-\frac{2}{3}\Delta\alpha_h'|\mathcal{E}_{loc}|_\Omega^2 s_h^m=-\frac{2}{3}\Delta\alpha_h'L^2|\mathcal{E}_0|_\Omega^2 s_h^m+U_{\mathrm{mf}}, \tag{10}$$

where s_h^m is defined in Eq. (3) and L is the usual Lorenz-Lorentz local field correction factor. The first term on the right-hand side of Eq. (10) is the molecule-field torque interaction and U_{mf} is the mean-field contribution from neighboring LC molecules. Following Maier and Saupe [38], we have

$$U_{\mathrm{mf}} = \langle U_{hh} \rangle = -\left\langle \sum_n G_{hh}^{mn} s_h^m s_h^n \right\rangle = -\left(\sum_n G_{hh}^{mn} \right) \langle S_h \rangle s_h^m = -\frac{u_{hh}}{3} \frac{Q_h}{N_h} s_h^m, \tag{11}$$

where $G_{hh}^{mn} s_h^m s_h^n$ denotes the orientational interaction energy between the mth and nth host molecules and

$$u_{hh} \equiv 3 \sum_n G_{hh}^{mn}. \tag{12}$$

We then find

$$\Delta \alpha_h' |\mathcal{E}_{loc}|_\Omega^2 = \Delta \alpha_h' L^2 |\mathcal{E}_0|_\Omega^2 + \frac{1}{2} u_{hh} \frac{Q_h(\Omega)}{N_h}. \tag{13}$$

From Eqs. (9) and (13), we obtain

$$Q_h(\Omega) = \frac{\gamma(\Omega)}{[1 - \gamma(\Omega) u_{hh}/2\Delta \alpha_h' N_h]} L^2 |\mathcal{E}_0|_\Omega^2. \tag{14}$$

In order to find $Q_h(\Omega)$, one needs to know $\gamma(\Omega)$, defined in Eq. (9). Reference [42], following Zwanzig's approach [54], uses a series expansion beyond the mean-field approximation to obtain $\gamma(\Omega)$. In the calculation, the orientational distribution of the LC molecules is also subjected to a diffusion equation like the one in Eq. (4), except for an additional driving term on the right-hand side proportional to U_{hh}. Equation (14) then becomes

$$Q_h(\Omega) = \frac{\Delta \alpha_h' L^2 N_h}{k_B T} \sum_k \frac{C_k}{1 - i\Omega \tau_k} |\mathcal{E}_0|_\Omega^2, \tag{15}$$

where the index k denotes the order of terms in the series expansion, with C_k describing their strengths and τ_k their orientational relaxation times. The $k=1$ term represents the mean-field contribution, with $C_1 \propto T/(T-T^*)$ and $\tau_1 = T/6D_h(T-T^*)$, where $T^* = u_{hh}/15k_B$ is the fictitious second-order phase transition (which is usually about 1 K below the actual nematic-isotropic phase transition temperature T_{ni}). Both C_1 and τ_1 exhibit the characteristic pretransitional behavior. The $k \geqslant 2$ terms come from going beyond the mean-field approximation in the expansion and represents more individual molecular characteristics, exhibiting no critical pretransitional behavior. Fourier transform of Eq. (15) yields immediately the time-dependent equation for Q_h

$$Q_h(t) = \frac{\Delta \alpha_h' L^2 N_h}{k_B T} \sum_k \frac{C_k}{\tau_k} \int_{-\infty}^t |E_0|^2(t') e^{-(t-t')/\tau_k} dt'. \tag{16}$$

The above equation describes the reorientational dynamics of the pure LC. If terms with $k \geqslant 2$ are neglected in Eq. (16), then it is identical to that obtained from the Landau-de Gennes theory [36,37].

With dye doping of the LC, the situation is modified. The reorientational potential seen by the LC molecules now consists of not only U_{hh}, but also of U_{he} and U_{hg} for interactions between the host LC molecules and the excited-state and ground-state dye molecules, respectively. Similar to U_{hh} in Eq. (11), they are defined as

$$U_{he} = -\sum_n G_{he}^{mn} s_h^m s_e^n, \quad U_{hg} = -\sum_n G_{hg}^{mn} s_h^m s_g^n. \tag{17}$$

In the mean-field approximation, we now have

$$U_{\mathrm{mf}} = \langle U_{hh} + U_{he} + U_{hg} \rangle = -\sum_{i=g,e,h} \frac{u_{hi}}{3} \frac{Q_i}{N_t} s_h^m,$$

$$u_{hi} \equiv \frac{3N_t}{N_i} \sum_n G_{hi}^{mn}, \tag{18}$$

with $N_t = N_h + N_e + N_g$ being the total molecular density of the sample. The factor 3 in the definition of u_{hi} above is to make it equivalent to that defined in Ref. [20]. We then find from Eq. (10)

$$\Delta \alpha_h' |\mathcal{E}_{loc}|_\Omega^2 = \Delta \alpha_h' L^2 |\mathcal{E}_0|_\Omega^2 + \frac{1}{2} u_{hh} \frac{Q_h(\Omega)}{N_t} + \frac{1}{2} u_{he} \frac{Q_e(\Omega)}{N_t} + \frac{1}{2} u_{hg} \frac{Q_g(\Omega)}{N_t}. \tag{19}$$

Accordingly, Eq. (16) becomes

$$Q_h^{dye\text{-}doped}(t) = Q_h^{pure}(t) + Q_h^{enh}(t),$$

with

$$Q_h^{pure}(t) = \sum_k \left(\frac{C_k}{\tau_k} \right) \int_{-\infty}^t BI(t') e^{-(t-t')/\tau_k} dt',$$

$$Q_h^{enh}(t) = \sum_k \left(\frac{C_k}{\tau_k} \right) \int_{-\infty}^t [u_{he} Q_e(t') + u_{hg} Q_g(t')] e^{-(t-t')/\tau_k} dt', \tag{20}$$

where $B = 4\pi L^2 \Delta \alpha_h' N_t / nc$, $I(t) = (nc/2\pi)|E_0|^2(t)$ is the optical pump intensity, and we have absorbed a factor of $1/(2k_BT)$ into the C_k's. Equations (20) and (8) completely describe the rotational dynamics of the dye-doped LC system.

C. Transient and steady-state enhancement

We can now discuss how excitation of dye molecules can affect the reorientation dynamics of LC molecules. In Eq. (20), we see that beside the optical torque on the LC molecules, represented by $BI(t)$, there are also torques that come from orientational anisotropies of dye molecules, i.e., the terms $u_{he} Q_e(t)$ and $u_{hg} Q_g(t)$. The latter show that reorientation effect of Q_e and Q_g on the LC molecules is gauged by the mean-field potentials u_{he} and u_{hg}, respectively, exerted on the LC molecules by the dye molecules in the excited and ground states. From Eq. (8), we see that $Q_e(t)$ and $Q_g(t)$ have opposite signs, and depending on the relative magnitudes of the two, the extra torques can enhance or reduce the reorientation caused by the optical torque. In other words, there is a competition between the excited-state and ground-state dye

population in reorienting the host LC molecules: $Q_e(t)$ wants to help align the LC molecules parallel to the optical field whereas $Q_g(t)$ wants to align them perpendicular to the optical field. For quantitative discussion of how dye molecules affect optical reorientation of LC, we define an enhancement factor $\eta(t)$ as

$$\eta(t) = Q_h^{dye\text{-}doped}(t)/Q_h^{pure}(t). \tag{21}$$

To have a feel of how the enhancement factor varies with time following pulsed laser excitation, we need to know the values of various time constants involved. As will be shown later, the relaxation times τ_{Qe} and τ_{Dg} for the dye are in the range of several hundreds of picoseconds (ps), while τ_k's for the LC range from picoseconds to tens of nanoseconds (ns). With the excitation pulse width of $\sim$10 ps, much shorter than the various dye relaxation times, we have Q_e and Q_g build up to Q_o and $-Q_o$ near the end of the pulse with $Q_o \equiv A\int_{-\infty}^{\infty} I(t)dt$. Soon after the pulse is over, Q_e and Q_g, following Eq. (8), decay as

$$Q_e(t) \simeq +Q_o e^{-t/\tau_{Qe}},$$

$$Q_g(t) \simeq -Q_o[(1+rF)e^{-t/\tau_{Dg}} - rFe^{-t/\tau_{Qe}}], \tag{22}$$

where $r \equiv \tau_{Qe}\tau_{Dg}/[\tau_f(\tau_{Qe}-\tau_{Dg})]$, and $t=0^+$ is taken as the time right after the pump pulse is essentially over. The direct effect of $Q_e(t)$ and $Q_g(t)$ on $Q_h(t)$, as governed by Eq. (20), lasts as long as they are nonzero, but their cumulative effect on $Q_h(t)$ persists. The enhancement factor η should start at 1 before the pump pulse arrives or before Q_e and Q_g come into play; then it becomes greater or less than 1 as Q_e and Q_g evolve, depending on whether the excited state or the ground state of the oriented dye molecules dominates in aligning the host molecules; and finally, it approaches a steady-state value as $Q_e(t)$ and $Q_g(t)$ decay to 0. Knowing that the relaxation times for $Q_e(t)$ and $Q_g(t)$ are in the hundreds of ps range, we expect the steady-state value of η will be reached at $\sim$1 ns after the pulsed excitation.

Under the assumption that the excitation pulse width is much shorter than the dye relaxation times τ_{Qe} and τ_{Dg}, and taking $F=1$, we have from Eq. (20), for $t \gg \tau_k$ for $k \geq 2$, the approximate result,

$$\begin{aligned} Q_h^{dye\text{-}doped}(t) \approx BC_1 e^{-t/\tau_1}\Bigg\{ 1 + \frac{A}{B}[&u_{he}\tau_{Qe}(1-e^{-t/\tau_{Qe}}) \\ &- u_{hg}\tau_{Dg}(1+r)(1-e^{-t/\tau_{Dg}}) \\ &+ u_{hg}\tau_{Qe}r(1-e^{-t/\tau_{Qe}})]\Bigg\}, \end{aligned} \tag{23}$$

and accordingly,

$$\begin{aligned} \eta(t) = 1 + \Bigg\{ \frac{A}{B}[&u_{he}\tau_{Qe}(1-e^{-t/\tau_{Qe}}) - u_{hg}\tau_{Dg}(1+r)(1-e^{-t/\tau_{Dg}}) \\ &+ u_{hg}\tau_{Qe}r(1-e^{-t/\tau_{Qe}})]\Bigg\}. \end{aligned} \tag{24}$$

For $t \gg \tau_{Qe}, \tau_{Dg}$, the above expression reduces to the steady-state form

$$\eta(t) \to \eta_\infty = 1 + \frac{A}{B}u_{he}\tau_{Qe}\left[1 - \frac{u_{hg}}{u_{he}}\frac{\tau_{Dg}}{\tau_{De}}\right]. \tag{25}$$

As can be seen from Eqs. (20) and (21), the same steady-state enhancement factor is obtained if pump pulses with pulse width much longer than τ_{Qe} and τ_{Dg} are used. This steady-state enhancement factor is the same as the one derived by Marrucci *et al.* [20]. In the experiment, we can obtain η_∞ in two ways: (i) by looking at $\eta(t)$ at a time much larger than τ_{Qe} and τ_{Dg} after a short pulse excitation and (ii) by measuring η with an optical pulse much longer than τ_{Qe} and τ_{Dg}. This is what we did in our experiment as will be described later.

It is seen from Eqs. (24) and (25) that η is larger or smaller than 1 depending on the relative magnitude of $u_{he}\tau_{De}$ and $u_{hg}\tau_{Dg}$, which are governed by the difference in how excited-state and ground-state dye molecules interact with the surrounding host LC molecules. The first excited electronic state of the anthraquinone dye used in our study is known to be a charge-transfer state [55]. Dye molecules in this state are expected to have a stronger interaction with the cyanobiphenyl host molecules than those in the ground state. The guest-host interactions also make the rotational diffusion time of the excited state longer. Together, they yield an enhancement factor larger than 1.

To date, only quasi-steady-state investigations of the enhanced optical reorientation in dye-doped LC system, using laser pulses of width $\sim$10 ns or longer, have been carried out. They measured the quantity η_∞. Their results agree with the prediction of the Jánossy's model, presented in this section. However, a dynamic study of the system should provide a much more stringent test of the model because of the added complexity. A recent work [26] looked at the transient rotational response of the dye molecules within the LC host and found that τ_{De} is significantly larger than τ_{Dg}, indicating a stronger excited dye-host interaction than the ground-state dye-host interaction. For a complete understanding of the guest-host interaction, one ought to measure not only the dynamic response of the guest but more importantly, also the dynamic response of the host. In our study reported here, we designed and performed a set of measurements to probe the rotational dynamics of the dye-doped LC system, governed by Eqs. (8) and (20). They are described in Sec. III.

III. EXPERIMENTS

A. General considerations

In our study, the guest-host system was isotropic pentylcyanobiphenyl (5CB) at 50 °C, unless otherwise noted, (T_{ni}=35.3 °C), doped with 0.05% by mass of the dye 1-amino-anthraquinone (1AAQ), which yields a number ratio $\sim$1:2000 of dye to LC molecules ($N_t \simeq N_h = 2.39\times10^{21}$ cm^{-3}, $N_d = 1.33\times10^{18}$ cm^{-3}). The 1AAQ dye was purchased from Aldrich, 5CB from Merck and Aldrich, and both were used without further purification. The samples were held in quartz cells of 1 mm thickness. The molecular structures of 5CB and 1AAQ and the absorption and fluorescence curves of 1AAQ are shown in Fig. 1. The material 5CB is transparent in the visible up to the near-UV range. In

the experiments, the dye molecules were excited into the first excited state centered around 475 nm; the transition has a transition dipole moment approximately parallel to the three-ring backbone of 1AAQ [55]. Depopulation of the first excited state is mainly through nonradiative decay—radiative decay only accounts for a few percent, and conversion to the triplet state is negligible [56].

To experimentally investigate the rotational dynamics of the guest-host system, we employed several implementations of the optical pump-probe scheme. In such an experiment, a linearly polarized pump beam is used to create the orientational anisotropies Q_i, followed by a time-delayed probe beam that measures the relaxation of the anisotropies and, hence, the rotational dynamics of the system [33,57]. Denoting the polarization direction of the pump beam as $\hat{n}$ and the laboratory coordinates as $u,v=x,y,z$, the orientational ordering of the system is described by

$$Q_i^{uv} = [(3/2)n_u n_v - (1/2)\delta_{uv}]Q_i. \tag{26}$$

If $\hat{n}$ lies in the $\hat{x}-\hat{z}$ or $\hat{y}-\hat{z}$ planes, then the anisotropy seen by a probe pulse propagating along $\hat{z}$ is

$$\begin{aligned}\Delta n(t) &\equiv n_x - n_y \\ &= \Delta n' + i\Delta n'' \\ &= \frac{4\pi L^2}{3n_o}\sum_{i=g,e,h}(\Delta\alpha_i' + i\Delta\alpha_i'')[Q_i^{xx}(t) - Q_i^{yy}(t)]. \end{aligned}\tag{27}$$

Here n_o is the refractive index of the isotropic system, and $\Delta\alpha_i' + i\Delta\alpha_i''$ is the complex polarizability anisotropy of the i-type molecular species at the probe wavelength. The $\Delta\alpha_i'$ and $\Delta\alpha_i''$ terms in Eq. (27) describe, respectively, the induced birefringence and induced dichroism.

In order to quantitatively understand the guest-host orientational dynamics, as described by Eq. (20), we need to separately characterize the rotational dynamics of each of the three molecular species in the dye-doped LC system. We outline here the set of experiments that were carried out to achieve our goal. First, we performed a quasi-steady-state pump-probe measurement on the system to determine the steady-state enhancement factor η_∞ and to look at the pump-wavelength dependence of the enhancement. Then we used different pump-probe schemes to measure transient fluorescence and dichroism to characterize the rotational dynamics of the dye responses, determining τ_f, τ_{Qe}, and τ_{Dg}. Finally, we adopted the pump-probe scheme of transient grating to look at the rotational dynamics of both the dye-doped LC and the pure LC systems. Knowing the relevant time responses of the dye molecules, we could fit the transient grating result and verify the model presented in the previous section.

The quasi-steady-state measurement was carried out using ~20-ns pulses generated from an optical parametric oscillator (OPO) pumped by a Q-switched Nd: yttrium-aluminum-garnet (YAG) laser. The time-resolved measurements were carried out using 14-ps pulses derived from a mode-locked Nd:YAG laser and an optical parametric system. In all of our experiments, when comparing the orientational nonlinearity between the pure and dye-doped LC materials, the attenuation of the pump beam in the dye-doped sample was taken into account by normalizing the observed signal against the average pump intensity in the sample. In all experiments, the pump intensity was verified to be below the saturation limit by varying the intensity above and below the used value and observing no change to the normalized signal. Section III B describes in details the experiments and the results found. A general discussion of the results is presented in Sec. IV.

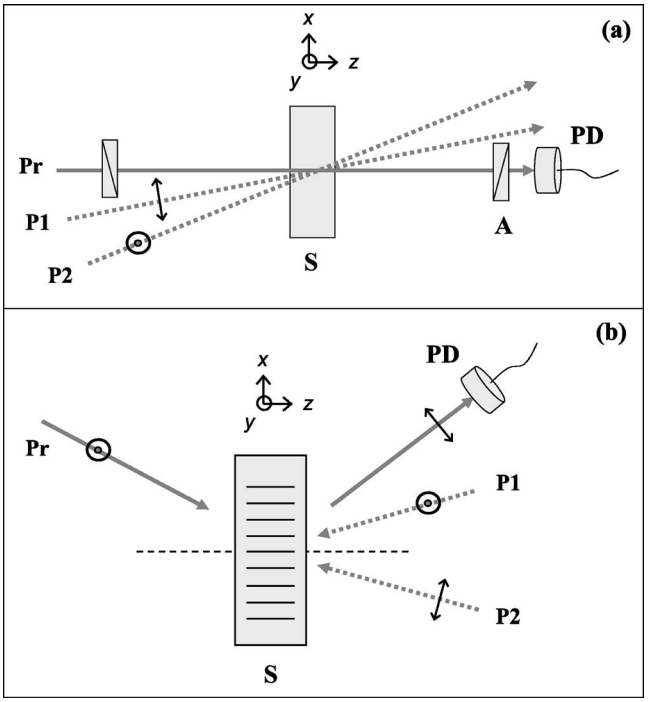

FIG. 2. Top-view schematic of the experimental setups. Pr: probe beam; $P1$, $P2$: pump beams #1 and #2; S: sample; PD: photodetector. All beams lie on the $\hat{x}-\hat{z}$ plane, with $P1$ and $P2$ polarized as shown. (a) Quasi-steady-state pump-probe and transient dichroism experiments. Input polarization of Pr is set to be along $\hat{x}+\hat{y}$, and analyzer A is set at or near $-\hat{x}+\hat{y}$. Signal is from Pr leaking through analyzer A as the pump beams induce optical anisotropy in the sample S. (b) Transient grating experiment. $P1$ and $P2$ form polarization grating at the sample, which diffracts s-polarized Pr as the p-polarized signal at the Bragg angle.

B. Experimental details and results

1. Quasi-steady-state enhancement

We first measured the steady-state enhancement factor η_∞ associated with the optical Kerr nonlinearity of the dye-doped LC system, and its pump-wavelength dependence over the lowest absorption band of the dye at ~475 nm. The measured pump-wavelength dependence of η_∞ is a check on the physical picture of the model, since according to Eq. (25), $(\eta_\infty - 1) \propto A$ is proportional to the absorption coefficient, but some previous wavelength-dependent measurements have found deviations from this proportionality [13,14]. The setup is shown schematically in Fig. 2(a), where pump beam $P1$ consists of wavelength-tunable ns pulses from the OPO (max energy ≃5 mJ), and probe beam Pr comes from a

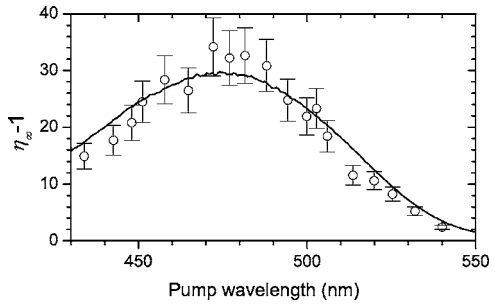

FIG. 3. Steady-state enhancement factor versus pump wavelength. Solid line is the scaled absorption spectrum.

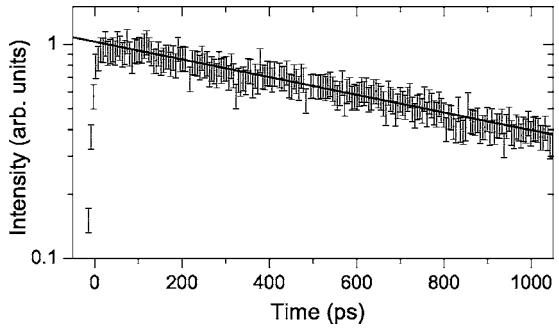

FIG. 4. Fluorescence intensity, polarized at the magic angle with respect to the pump beam polarization versus time. Solid line is single exponential fit.

10 mW cw HeNe laser, having diameter of 3 mm and 0.5 mm, respectively, and coming together at an angle of about 5°. (Pump beam $P2$ was not utilized in this experiment.) The two beams, $P1$ and Pr, are polarized along $\hat{y}$ and $\hat{x}+\hat{y}$ before the sample, and the analyzer transmission axis is set at the crossed position along $-\hat{x}+\hat{y}$. In the absence of the pump pulse, the analyzer completely blocks the probe beam. The pump pulse induces an optical anisotropy Δn, causing the probe beam to leak through the analyzer and appear as a signal: $S \propto |\Delta n|^2$. In this quasi-steady-state case, the contribution from the dye to the signal is negligibly small [19,21]. Comparison of the signals obtained from the pure and the dye-doped LC samples readily yields η_∞ [21].

Figure 3 presents the result of the quasi-steady-state measurement of the dye-doped LC system. The factor $(\eta_\infty - 1)$ measured at $T=38$ °C, and the linear absorption of the dye-doped LC are plotted as functions of the pump wavelength. As expected, $(\eta_\infty - 1)$ follows the absorption spectrum. This confirms the picture that the enhancement comes from excitation of dye molecules into the charge-transfer S_1 state, agreeing with the result found in a recent study [15].

2. Dynamic response of dye molecules

We next embarked on measuring the dynamic response of the dye molecules, as characterized by the time constants τ_f, τ_{Qe}, and τ_{Dg}. To find the lifetime τ_f of the dye-excited state, we utilized the transient fluorescence scheme where linearly polarized ps pulses at 532 nm from a Nd:YAG laser system excited the dye molecules in the dye-doped LC sample, and the subsequent time-dependent fluorescence signal is monitored through an optical-Kerr shutter [58] gated by 1064-nm pulses from the same Nd:YAG laser system. This transient fluorescence technique was described in detail elsewhere [59]. The fluorescence was measured at the "magic" polarization angle of 54.7° with respect to the pump polarization so that it was independent of the orientational distribution of the excited molecules. It then yielded a single exponential decay with decay time τ_f [59]. The result is shown in Fig. 4, from which we deduced $\tau_f = 1050 \pm 60$ ps [63]. In principle, if we measure, separately, fluorescence polarized parallel $(I_\parallel)$ and perpendicular $(I_\perp)$ to the pump polarization, then since $[I_\parallel(t) - I_\perp] \propto e^{-t/\tau_{Qe}}$, τ_{Qe} could be deduced [59]. However, this procedure requires that $I_\parallel$ and $I_\perp$ be properly normalized to each other, a task that is not easy to be accurate and could introduce large uncertainty in the deduced value of τ_{Qe} [59,63]. Therefore, we opted for a different method to find τ_{Qe}, which is described below.

To probe the rotational dynamics of dye both in the excited and ground states, we employed a pump-probe scheme that measures transient dichroism. In the scheme, the dichroic part of the induced optical anisotropy can be probed separately from the birefringence part [Eq. (27)] [60,61]. It then allowed us to avoid complication due to induced birefringence in the 5CB host, which is transparent at pump and probe wavelengths and, therefore, does not contribute to the induced dichroism [28].

As depicted in Fig. 2(a), the pump pulse $P1$, incident on the sample at a small angle 5°, was p-polarized in the $\hat{x}-\hat{z}$ plane and the probe pulse Pr was polarized along $\hat{x}+\hat{y}$. The two pulses had energies of 20 and 2–6 μJ and beam diameters of 1 and 0.4 mm, respectively. Pump wavelength was set at 480 nm, near the absorption peak of the dye in the ground state. The analyzer [A in Fig. 2(a)] was set at a small angle γ away from the crossed position of $-\hat{x}+\hat{y}$. With this geometry, if the optical anisotropy is sufficiently small, the observed signal leaking through the analyzer is given by

$$S_t(\gamma,t) = S_o\left\{\left[\frac{\pi l}{\lambda}\Delta n''(t) - \gamma\right]^2 + \left[\frac{\pi l}{\lambda}\Delta n'(t)\right]^2\right\}, \quad (28)$$

where $S_o \equiv S_{in} e^{-4\pi l n_o''/\lambda}$ with S_{in} being the incident probe intensity, λ the probe light wavelength, and l the sample thickness. Equation (28) is a parabolic function of γ with $(\pi l/\lambda)\Delta n'(t)$ and $(\pi l/\lambda)\Delta n''(t)$ describing the position of the minimum on the ordinate and the abscissa axes, respectively. Thus, by measuring S_t versus γ and fitting to find the minimum position, as shown in Fig. 5(a), we can determine $\Delta n''$ separately from $\Delta n'$.

To focus on the time evolution of the induced dichroism, and, hence, the rotational dynamics of the solute, we measured $S(t) \equiv S_t(-\gamma,t) - S_t(\gamma,t)$ and obtain

$$S(t) = S_o \frac{4\pi l}{\lambda}\gamma\Delta n''(t) = (2\gamma l S_o/3n_o)\sum_{i=g,e}\Delta\sigma_i[Q_i^{xx}(t) - Q_i^{yy}(t)], \quad (29)$$

where $\Delta\sigma_i \equiv \sigma_{i,\parallel} - \sigma_{i,\perp} = (8\pi^2/\lambda)\Delta\alpha_i''$ denoting anisotropy in the absorption cross section of dye molecules in state i, with the parallel direction referring to the long molecular axis.

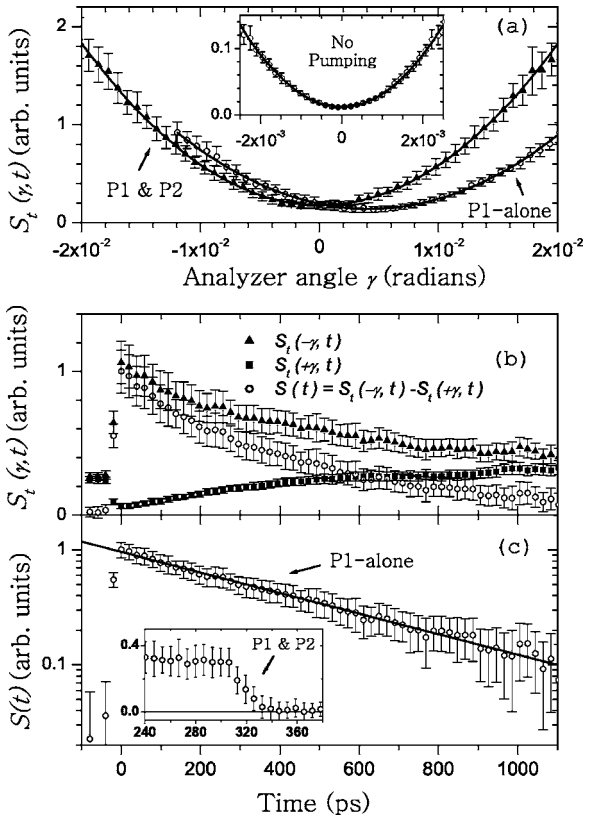

FIG. 5. Dye excited-state dichroism probed at 600 nm. (a) $S_t(\gamma,t)$ versus γ at $t=340$ ps, induced by pump pulse $P1$ alone (at $t=0$) and by pump pulse $P1$ followed by time-delayed pump pulse $P2$ (at $t=320$ ps) that reduces the excited state dichroism to zero. The dichroism is determined from the abscissa of the fitted parabolic minimum, which appears at $\gamma=0$ in the absence of the pump pulse (inset). The $P1$-alone and $P1$ with $P2$ scans yielded the minimum abscissa at $4.2\pm0.16\times10^{-3}$ and $0\pm1.5\times10^{-4}$ rad, respectively, showing that the excited state dichroism is nullified to better than ±4%. (b) Transient dichroism signal $S(t)$ measured by taking the difference between the heterodyned signals $S_t(-\gamma,t)$ and $S_t(+\gamma,t)$. (c) Single exponential fit of the same excited-state dichroism data $S(t)$ shown in (b). The inset shows how the dichroism induced by $P1$ is reduced to zero by $P2$.

Note that the induced dichroism could be positive or negative. An example is shown in Fig. 5(b).

Equation (29) shows that if there is a probe wavelength range where $\Delta\sigma_e$ or $\Delta\sigma_g$ is negligible compared to the other, then the state-specific dichroism, and, hence, the corresponding rotational dynamics, of the other can be measured. It is often possible to find at selected wavelengths that $\Delta\sigma_g \ll \Delta\sigma_e$, but not the reverse. Then probing the excited-state rotational dynamics is easy, but not so for the ground state. One might think that the ground-state rotational dynamics could be deduced from the measured $S(t)$ of Eq. (29) at a wavelength where both $\Delta\sigma_e$ and $\Delta\sigma_g$ are nonvanishing if the excited-state rotational dynamics and $\Delta\sigma_e/\Delta\sigma_g$ are known. Unfortunately, determination of $\Delta\sigma_e/\Delta\sigma_g$ is often complicated by model dependence and simultaneous contributions from absorption and stimulated emission to $\Delta\sigma_e$, yielding scattered results in the literature [62]. Thus, in order to measure the ground-state rotational dynamics, we must

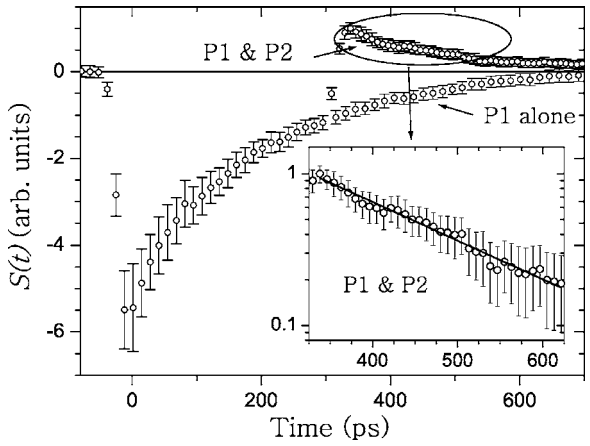

FIG. 6. Transient dichroism probed at 505 nm, induced by pump pulses $P1$ at $t=0$ ps and $P2$ at $t=320$ ps. After $P2$, the observed dichroism reverses sign and decays exponentially. The inset shows the single-exponential fit of the experimental data after $P2$.

eliminate the contribution from the excited state in the induced dichroism measurement. We have recently devised a method employing two pump pulses to accomplish this [28].

As shown in Fig. 2(a), we used a second pump pulse $P2$ to irradiate the sample at $t=t_D$ following the first pump pulse $P1$ at $t=0$, both of the same wavelength. With $P1$ polarized along $\hat{n}$ in the $\hat{x}-\hat{z}$ plane, the induced anisotropy in the excited state of the dye molecules is $(Q_e^{xx}-Q_e^{yy})_{t<t_D}=(3/2)(\hat{n}\cdot\hat{x})^2Q_oe^{-t/\tau_{Qe}}$. If $P2$ is polarized along $\hat{y}$ with a proper intensity, then it can generate an opposite orientational anisotropy in the excited state to completely cancel $(Q_e^{xx}-Q_e^{yy})_{t=t_D}$, yielding $[Q_e^{xx}-Q_e^{yy}]_{t>t_D}=0$. Thus, the excited state no longer contributes to the dichroism, but if $\tau_{Dg}\neq\tau_{De}$, then the ground-state dichroism survives. We have from Eqs. (22), (26), and (29)

$$\begin{aligned} S(t>t_D) &\propto [Q_g^{xx}-Q_g^{yy}](t>t_D) \\ &= (3/2)(\hat{n}\cdot\hat{x})^2Q_o(1+rF)e^{-t_D/\tau_{Qe}} \\ &\quad\times\{1-\exp[t_D(\tau_{Dg}-\tau_{Qe})/\tau_{Dg}\tau_{Qe}]\}e^{-(t-t_D)/\tau_{Dg}}, \end{aligned} \tag{30}$$

which is a single exponential decay characterized by the ground-state rotational diffusion time τ_{Dg}.

The results of our transient dichroism measurements are presented in Figs. 5 and 6. The dichroism signal was normalized pulse by pulse against the probe pulse energies, and the fluctuations of the pump were limited to less than 12%. Each data point shown was the result of averaging over 100 pulses. To selectively probe the excited-state rotational dynamics of 1AAQ, the probe wavelength was set at 600 nm, below the ground-state absorption band. The induced dichroism by $P1$ only should decay exponentially with a time constant of τ_{Qe}. The experimental result is displayed in Figs. 5(b) and 5(c), from which we deduce $\tau_{Qe}=490\pm30$ ps [63]. Knowing $\tau_f=1050\pm60$ ps from the fluorescence measurement, we find $\tau_{De}=900\pm110$ ps, agreeing within experimental error with the value reported by Paparo *et al.* [64]. {From our earlier work [27], we have also

obtained the relative magnitudes of the excited absorption anisotropy at three different probe wavelengths in the near-infrared: $\Delta\alpha_e''(925\text{ nm})/\Delta\alpha_e''(848\text{ nm}) \simeq 0.4$, $\Delta\alpha_e''(1024\text{ nm})/\Delta\alpha_e''(848\text{ nm}) \simeq 0$, with uncertainty at about 15%. These results will be used to corroborate our fitting of the overall optical anisotropy of the guest-host system, as described later.}

At all possible wavelengths to probe ground-state dichroism of 1AAQ, the excited-state absorption is significant. We used the two-pump-pulse scheme with $t_D=320$ ps to eliminate the excited-state contribution. As shown in Fig. 5(a), with a proper $P2$ intensity, the excited-state anisotropy $Q_e^{xx}-Q_e^{yy}$, selectively monitored by the probe beam at 600 nm, could be nullified to better than ±4% soon after $t=t_D$. Then with the same sequential $P1$ and $P2$ pulses, we could probe the ground-state dichroism using probe pulses at 505 nm, which is inside the ground-state absorption band. The result is shown in Fig. 6. We see that for $t<t_D$, the induced dichroism is negative as it is dominated by oriented ground-state bleaching, and for $t>t_D$, pulse $P2$ reversed the sign of the dichroism, as expected from Eq. (30) for $\tau_{Dg}<\tau_{De}$. The exponential decay of the dichroism after t_D yields $\tau_{Dg}=170\pm20$ ps.

Summarizing the results of our measurements on the rotational dynamics of 1AAQ in 5CB, we have found that for the excited state of 1AAQ, $\tau_f=1050\pm60$ ps, $\tau_{Qe}=490\pm30$ ps, and $\tau_{De}=900\pm110$ ps, and for the ground state, $\tau_{Dg}=170\pm20$ ps. The rotational diffusion time of the excited state is markedly longer than that of the ground state, signifying a stronger guest-host frictional force upon dye excitation, as have been found in previous state-specific rotational dynamics studies of various solute-solvent systems [26,65]. As seen through Eq. (25), the longer rotational diffusion time of the excited dye molecules contributes to a positive enhancement in the field-induced reorientation of the LC host molecules. Thus, the result of our rotational dynamics measurements on 1AAQ in 5CB provides an independent confirmation on the change of guest-host interaction upon excitation of the guest that affects the light-induced reorientation of the host molecules, which is the central assumption of the current model explaining the Jánossy effect.

3. Reorientational dynamics of the guest-host system

With the rotational dynamics of the dye characterized, we then proceeded to probe the overall rotational dynamics of the guest-host system using the pump-probe transient grating scheme [66,67]. A schematic of the setup is shown in Fig. 2(b). Two ps pump pulses, $P1$ and $P2$, at 532 nm with s and p polarizations, respectively, and each with energy of 40 μJ/pulse, overlapped at an angle of 14° over a spot of ~3.5 mm in diameter on the sample and formed a polarization grating that induced a transient refractive index grating in the medium. The time-delayed s-polarized probe pulse Pr with wavelength λ_{probe}, beam diameter of 1 mm, and energy of 1 μJ/pulse was used to probe the transient grating by Bragg diffraction and the p-polarized diffracted output $S(t)$ was recorded.

It is known that the diffracted signal from a grating of complex refractive index is given by [67]: $S\propto|\delta n|^2$, where δn is the contrast between the minima and maxima of the complex refractive index grating. Because the field intensity is uniform across the polarization grating and only the polarization of the field varies, such a grating produces no thermal or acoustic effects normally associated with intensity gratings which could complicate data analysis. The contrast δn is directly proportional to Δn given in Eq. (27) [67]. Hence, with $I_{pr}(t)$ being the time-varying intensity of the probe pulse, the time-dependent diffraction signal is

$$S(t) \propto \int_{-\infty}^{\infty} I_{pr}(t-t')|\Delta n(t')|^2 dt'. \tag{31}$$

Our main goal is to observe the reorientation of the LC molecules due to the optical pulse with and without the presence of the dye. Thus, we want to minimize the contribution of the dye to the overall signal by choosing appropriate probe wavelengths to minimize $\Delta\alpha_g$ and $\Delta\alpha_e$ in Eq. (27). Therefore, we set the probe-wavelengths to be in the near-IR range, away from the resonant transitions of the dye from the ground and excited states. The observed signal from a pure LC sample at $\lambda_{probe}=848$ nm and a dye-doped sample at $\lambda_{probe}=848$, 925, and 1024 nm are displayed as the square root of S versus t [for convenience of visualizing $\Delta n(t)$ versus t approximately] in Figs. 7(a)–7(d). The time variations of S from the pure LC sample were the same for the three λ_{probe}'s, and the amplitude of the dye-doped signals shown in

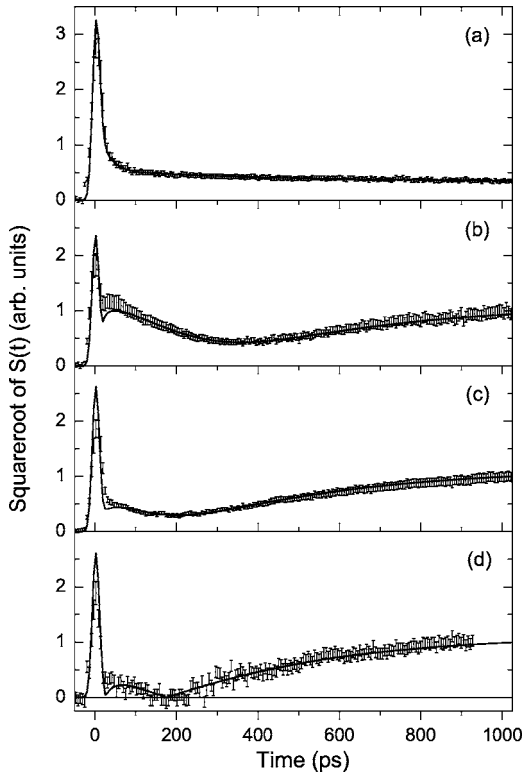

FIG. 7. Result of the transient grating experiment from (a) pure LC at probe wavelength of 848 nm and from dye-doped LC at (b) 848 nm, (c) 925 nm, and (d) 1024 nm. Solid lines are theoretical fits. The signal from dye-doped LC are fitted with $\eta_\infty=3.3$ and $r_u=0.6$. See text for fitting procedure.

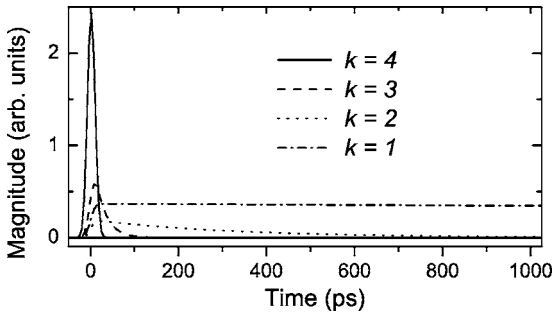

FIG. 8. The four components of $\Delta\alpha_h' Q_h^{pure}(t)$, described by Eq. (20), used to obtain the fit in Fig. 7(a) for the transient grating signal from pure LC. Vertical scale is the same as in Fig. 7.

Fig. 7 have been normalized against that of the pure sample at the same probe wavelengths. To characterize the response of our setup, we used a sample of benzene, whose response time of ~1 ps [68] could be approximated as being instantaneous in our case. Taking the same Gaussian time profile for both the pump and probe pulses, fitting of the transient signal from benzene according to Eq. (31) yielded a full width at half maximum pulse width of 14 ps for the pump and probe pulses. Comparing the signal from pure LC with that from benzene and knowing the nonlinearity of benzene [69], we estimated that the maximum $S(t)$ in Fig. 7(a) for pure LC corresponds to $Q_h \sim 1\times 10^{16}$ cm^{-3}, or an order parameter of $Q_h/N_h \sim 4\times 10^{-6}$.

We fitted quantitatively the observed $S(t)$ of pure LC in Fig. 7(a) using Eqs. (31) and (27), with $Q_h^{pure}(t)$ given in Eq. (20). Using the ns pump-probe setup, we measured the longest exponential decay time τ_1 of Q_h^{pure} and found $\tau_1 = 16.5\pm 0.8$ ns, which agrees with the result of Ref. [48]. From previous works [41,43,44,48,50], we know that the various exponential decay times τ_k of Q_h^{pure} differ in order of magnitude, so to find them we used a successive tail matching procedure. We started by fitting the long tail of $S(t)$ by the $k=1$ component alone in Eq. (20) with $\tau_1 = 16.5$ ns and C_1 as the adjustable parameter. The $k=1$ component was then subtracted out from the signal, and another tail matching was performed to determine the $k=2$ component, with τ_2 and C_2 as adjustable parameters, and similarly for the $k=3$ and $k=4$ components. Figure 8 shows the k components obtained from the fit, with $\tau_1 = 16.5\pm 0.8$ ns, $\tau_2 = 320\pm 60$ ps, $\tau_3 = 23.5\pm 5.0$ ps, $\tau_4 < 5$ ps, and $C_1/C_2/C_3/C_4 = 1/0.010/0.0041/0.0088$ with uncertainties of 5%, 10%, 20%, and 12%, respectively, and as seen in Fig. 7(a), the overall fit with the experimental curve is very good. The peak of the response curve at $t\sim 0$ in Fig. 7(a) would have a detectable shift if $\tau_4 \geqslant 5$ ps. The absolute magnitude of the signal from the pure sample was used as a scale factor for subsequent fitting of results from the dye-doped LC sample described below.

Turning our attention now to the signals from the dye-doped sample, shown in Figs. 7(b)–7(d), we see that $S(t)$ at the three λ_{probe}'s all roughly follow the same qualitative behavior: a sharp peak near $t=0$, similar to that of the pure signal, then a decrease through a minimum, and then a gradual increase to about the same magnitude for all three λ_{probe} at $t\simeq 1$ ns. The differences appear in the detailed behavior of $S(t)$ for $t \leqslant 700$ ps in magnitudes and positions of the minimum. They originate from significant contribution to $S(t)$ from the dye and from the dependence of $\Delta\alpha_g$ and $\Delta\alpha_e$ on λ_{probe}. As the dye contribution to $S(t)$ decays away for $t \geqslant 700$ (recall that $\tau_{Qe}=490$ ps and $\tau_{Dg}=170$ ps), the signal $S(t)$ becomes dominated by the LC host contribution, which is insensitive to λ_{probe}. Note that at $t\approx 1$ ns, $S(t)$ for the dye-doped LC is higher than that of the pure sample; this signifies the enhanced reorientation effect in the dye-doped LC case.

To understand quantitatively the signal from the dye-doped sample, we first note that at the chosen near-IR probe wavelengths, $\Delta\alpha_g'' = \Delta\alpha_h'' = 0$, and $\Delta\alpha_e''$ is small but nonvanishing. Knowing that $[Q_i^{xx}(t) - Q_i^{yy}(t)] \propto Q_i(t)$, we have from Eqs. (27) and (31),

$$S(t) \propto [\Delta\alpha_e' Q_e + \Delta\alpha_g' Q_g + \Delta\alpha_h' Q_h^{pure} + \Delta\alpha_h' Q_h^{enh}]^2 + [\Delta\alpha_e'' Q_e]^2, \tag{32}$$

where $Q_e(t)$ and $Q_g(t)$ are given by Eq. (8) and $Q_h^{pure}(t)$ and $Q_h^{enh}(t)$ by Eq. (20). Using the amplitude of the $k=1$ component of Q_h^{pure} as the normalization constant, we can use Eq. (32) to fit the experimental curves, taking $\Delta\alpha_e'/(\Delta\alpha_h' C_1)$, $\Delta\alpha_g'/(\Delta\alpha_h' C_1)$, $\Delta\alpha_e''/(\Delta\alpha_h' C_1)$, u_{hg}, and u_{he} as fitting parameters. The last two parameters appear in the expression of $Q_h^{enh}(t)$ in Eq. (20). Furthermore, we found that it is advantageous to replace u_{hg} and u_{he} with two dimensionless parameters: $r_u \equiv u_{hg}/u_{he}$ and η_∞ [Eq. (25)], which represent the ratio and (scaled) difference, respectively, of the mean-field interaction energies. It is known that $u_{hg} > 0$ from ground-state dichroism measurement of nematic-phase dye-doped LC samples [16], and we expect $u_{hg} \leqslant u_{he}$ from physical arguments discussed earlier [17,22]. Thus, the parameter r_u is restricted to the range $0 < r_u \leqslant 1$.

The values of $\Delta\alpha_e'$ and $\Delta\alpha_g'$ are expected to be of opposite sign to $\Delta\alpha_h'$. This is because the easy-polarizing axis for 1AAQ is along the C═O bonds, perpendicular to the molecular long axis. The presence of terms with opposite signs in the first square brackets of the right-hand side of Eq. (32) means that as time proceeds, $S(t)$ could go through a minimum if the birefringence terms in the first square brackets cancel each other, and the minimum would be $[\Delta\alpha_e'' Q_e]^2$ at that particular time. Indeed the observed $\sqrt{S(t)}$ for each probe wavelength, described in Figs. 7(b)–7(d), does go through a minimum at around 200–400 ps. The corresponding dichroism magnitude at minimum $\sqrt{S(t)}$ yields the relative magnitudes of the dye excited-state dichroism at the different probe wavelengths: $\Delta\alpha_e''(925\text{ nm})/\Delta\alpha_e''(848\text{ nm}) = 0.50$, $\Delta\alpha_e''(1024\text{ nm})/\Delta\alpha_e''(848\text{ nm}) = 0.0$, with uncertainty at 12%. These values agree within experimental error with what we found in the transient dichroism measurement described in the previous section.

Figure 9(a) shows the excited-state and ground-state dye anisotropies $Q_e(t)$ and $Q_g(t)$, as given by Eqs. (8) with $F=1$ and the various τ's experimentally determined previously. Note the negative sign on $Q_g(t)$. From $Q_e(t)$ and $Q_g(t)$ we can calculate the transient torque that reorients the LC

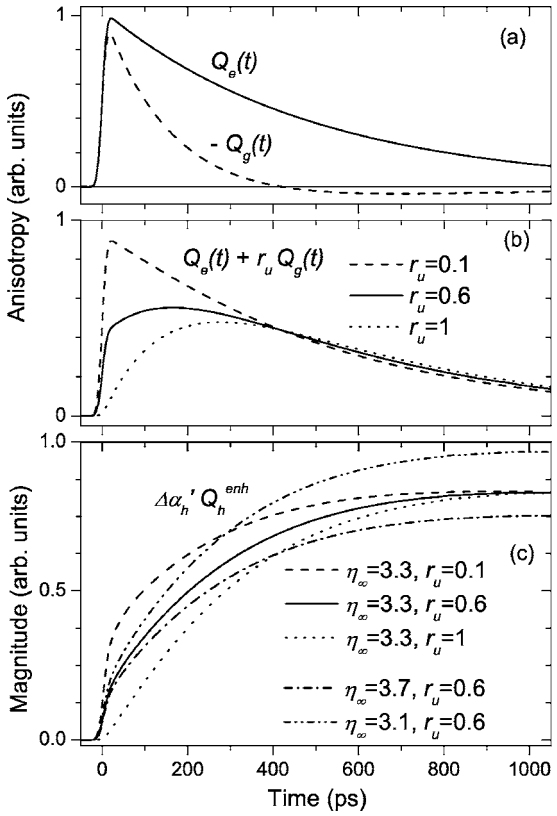

FIG. 9. Fitting of the dye torque: (a) Excited-state and ground-state dye anisotropies. Note the negative sign on $Q_g(t)$. (b) Net transient torque from the dye population acting on the LC host, represented by $Q_e(t)+r_uQ_g(t)$, for different values of r_u. (c) LC anisotropy created by the dye torque, $Q_h^{enh}(t)$, for different values of η_∞ and r_u. Vertical scale of (c) is the same as in Fig. 7.

host, as represented by the quantity $Q_e(t)+r_uQ_g(t)$ [refer to Eq. (20)]. The transient torque for different values of r_u is shown in Fig. 9(b). Representative curves for $Q_h^{enh}(t)$, as a result of the dye excitation [Eq. (20)], with different values of η_∞ and r_u, are shown in Fig. 9(c). We see that η_∞, being the steady-state enhancement factor, determines the asymptotic value of $Q_h^{enh}(t)$ as t becomes much larger than τ_{Dg} and τ_{Qe} ($t \geqslant 800$ ps). As seen in Fig. 10(a), among the various terms described by Eq. (32) to compose $S(t)$, $\Delta\alpha_h' Q_h^{enh}$ is dominant in the time regime $t \geqslant 800$ ps that limits the range of possible values for η_∞. The best-fit value was $\eta_\infty = 3.3 \pm 0.4/0.2$.

The situation is different in determining r_u. Different values of r_u affect the net torque of dye on host molecules $[\propto Q_e(t)+r_uQ_g(t)]$ [Fig. 9(b)] mainly in the early time $t \leqslant 400$ ps because $Q_g(t)$ decays much faster than $Q_e(t)$ [Fig. 9(a)]. The subsequent effect of different r_u on $Q_h^{enh}(t)$ is moderate and also mainly in the early time $t \leqslant 600$ ps. In fitting of the measured signal $S(t)$ through Eq. (32), it turns out that the change of $Q_h^{enh}(t)$ due to different r_u could be offset by adjusting the values of the $\Delta\alpha_e'$ and $\Delta\alpha_g'$ to change the dye contribution, $[\Delta\alpha_e' Q_e(t)+\Delta\alpha_e' Q_g(t)]$, in Eq. (32). We found that any value of r_u within the range $0 < r_u \leqslant 1$ would yield a satisfactory fit. This is shown in Fig. 10(b), for r_u=0.1 and 1.

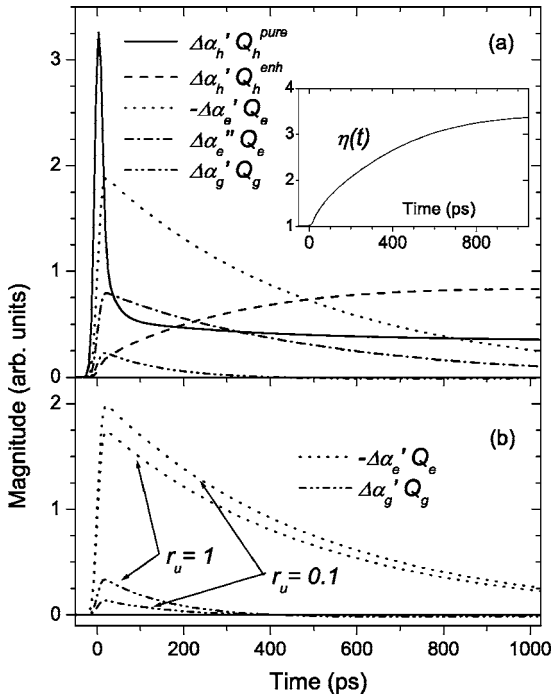

FIG. 10. Fitting of the transient grating signal from dye-doped LC: (a) The five terms, described by Eq. (32), used to obtain the fit in Fig. 7(b), where η_∞=3.3 and r_u=0.6. Note the negative sign on $\Delta\alpha_e' Q_e$. Inset of (a) gives the corresponding transient enhancement factor $\eta(t)$. (b) For different values of r_u, with the dye contribution to the signal adjusted as shown, the fit remains practically the same as in Fig. 7(b). Vertical scale is the same as in Fig. 7.

As seen in Figs. 7(b)–7(d) we obtained remarkably good fits between theory and experiment at all three probe wavelengths. The various terms of the fit, described in Eq. (32), for the case of λ_{probe}=848 nm [Fig. 7(b)] are shown in Fig. 10(a). The relative magnitudes of the dye polarizability anisotropies used to obtain the fits for the signal at all three probe wavelengths [Figs. 7(b)–7(d)] are listed in Table I. At these wavelengths, $\Delta\alpha_e'$ is significantly larger than the corresponding $\Delta\alpha_g'$ because it is near or at resonance, as demonstrated by the nonzero values of $\Delta\alpha_e''$. By comparing with the signal from benzene as mentioned earlier, the value of $\Delta\alpha_g'$ at 848 nm used in the fit of Fig. 7(b) is estimated to be $\simeq 2\text{Å}^3$, which is comparable to the values obtained for similar compounds [70]. The estimated value of $\Delta\alpha_e''$ at 848 nm corresponds to $\Delta\sigma_e \simeq 4.2\times10^{-18}$ cm^2 (for comparison, $\Delta\sigma_g = 1.5\times10^{-17}$ cm^2 at 532 nm).

From the fitting result of η_∞ and r_u, together with the material parameters of the 1AAQ/5CB system, we can

TABLE I. Relative magnitudes of dye polarizability anisotropies from the transient grating experiment, from the fits in Figs. 7(b)–7(d). $\Delta\alpha_g'$ at λ_{probe}=848 nm is estimated to be $\simeq 2$ Å^3.

	$\Delta\alpha_g'$	$\Delta\alpha_e'$	$\Delta\alpha_e''$
λ_{probe}=848 nm	1	7.4	3.2
925 nm	1.0	5.5	1.6
1024 nm	1.0	5.5	0.0

calculate u_{he} and u_{hg}. At $\lambda_{pump}=532$ nm, the linear absorption of the dye-doped sample is $\beta=6.8\ \mathrm{cm}^{-1}$, $n=1.58$, $\Delta\alpha_h'=17.6\text{Å}^3$ [34], yielding $A/B=4.65\times10^{10}\ \mathrm{eV}^{-1}\ \mathrm{s}^{-1}$ [71]. Then the result of $\eta_\infty=3.3\pm0.4/0.2$ and $0<r_u\leqslant1$ yields the following approximate range for the mean-field orientational energies: $0.090\leqslant u_{he}\leqslant0.17$ eV and $0<u_{hg}\leqslant0.17$ eV. These are comparable to the values measured and deduced in earlier studies of the Jánossy effect in similar anthraquinone-dye-doped LC systems [16,24]. We also found that if $F=0$ was assumed, no significant difference in the results of the fitting was found.

IV. DISCUSSION AND CONCLUSION

Theoretical fitting of the experiment allowed us to deduce the time-dependent reorientation enhancement $\eta(t)$ [Eqs. (20) and (21)]. As shown in the inset of Fig. 10(a), for a representative case of $\eta_\infty=3.3$ and $r_u=0.6$, $\eta(t)$ behaves as we expect: it starts at 1 at $t=0$, increases with time, corresponding to when the net extra torque resulting from $Q_e(t)$ and $Q_g(t)$ builds up, and asymptotically approaches the steady-state value as $Q_e(t)$ and $Q_g(t)$ decay away. The value $\eta_\infty=3.3\pm0.4/0.2$ we deduced from our transient measurements agrees with the value $\eta_\infty=3.0\pm0.3$ we obtained from the quasi-steady-state, nanosecond pump –probe measurement. Thus, we have elucidated the transition of the enhancement process from the transient regime to the quasi-steady-state regime.

The enhancement effect relies on two key features. Referring to the expression for η_∞ in Eq. (25), it first requires $(Au_{he}\tau_{Qe})/B\geqslant1$. The parameter A quantifies the absorption strength of the dye, u_{he} quantifies the orientational coupling between LC molecules and excited dye molecules, and τ_{Qe} quantifies the time window that the excited dye molecules exert a torque on the host, while B quantifies the direct optical torque. However, having a strong dye torque is not enough—it also requires that the overall reorientational effects of dye molecules in the excited and ground states on the host are different, which is represented by $(u_{hg}/u_{he})(\tau_{Dg}/\tau_{De})\neq1$. These two features combine to yield a η_∞ different from 1.

For the 1AAQ/5CB system, we have found that the ground-state dye anisotropy decays away significantly faster than the excited-state counterpart, $\tau_{Dg}/\tau_{De}=0.2$, so that the net dye-assisted reorientation of the LC host at later times is mainly due to the excited dye molecules, with less than 20% $[=r_u(\tau_{Dg}/\tau_{De})]$ counterbalanced by the negative action of the ground-state dye anisotropy. The contribution to the enhanced reorientation of the LC host from the change in rotational diffusion between the dye excited and ground states is so large that it masks out the contribution, if any, from the change in mean-field reorientational energies.

The observed decrease in rotational diffusion upon excitation of the dye in 5CB is the largest reported in the literature so far [26,65], but we note that our study is the first to directly probe the ground-state rotational dynamics of a dye [28]. As mentioned earlier, the first excited state of 1AAQ corresponds to an intramolecular charge-transfer state where electronic charge is transferred from the amino group to the carbonyl groups [55], making the amino group more prone to form a hydrogen bond with available hydrogen-bonding moieties of the surrounding solvent molecules such as the cyano group of 5CB [17,56]. Other possible modes of interaction between 1AAQ and 5CB, such as van der Waals or dipole-dipole interaction, are also expected to increase in strength upon excitation of 1AAQ due to the more extended electronic cloud distribution and dipolar characteristic of the excited state. This overall stronger interaction leads to an increase of frictional forces between the excited 1AAQ and neighboring 5CB molecules, impeding rotational diffusion of the excited molecules as compared with their ground-state counterpart. It has been shown before that large change in dye rotational diffusion could result from relative small change in the overall guest-host interaction energy [16,72]. According to Ref. [72], in the simplest approximation, the rotational diffusion constant depends on the guest-host interaction through the Arrhenius-type relation

$$D_{g,e}\propto\exp(-E/kT) \tag{33}$$

where E is the associated activation energy. For the temperature and material system used in this work, $E\sim10\ kT$ [16]; a change of $\sim15\%$ in E is enough to change $D_{g,e}$ by a factor of 5.

In both Ref. [16] and our study, the values of u_{hg} and u_{he} are ~0.2 eV, compared to the typical value $u_{hh}\sim0.4$ eV for the mean-field interaction of the host LC. They are consistent with the typical strength known for polar dipole-dipole and hydrogen-bonding interactions [35].

We have found good agreement between model prediction and experimental data in our time-resolved study of the Jánossy effect, thus significantly expanding our confidence in the model. The same physical underpinnings of the model apply to dye-doped LC in the nematic phase [19–21]. It has been suggested that a change in rotational diffusion upon photoexcitation, as observed in our study, could also be the driving force in the optical reorientation of azo-dye systems, working either in conjunction with or, in certain cases, instead of the well-known photoisomerization of the azo dyes [26]. In fact, several azo dye-doped LC systems have been found to exhibit enhanced optical reorientation [12,14]. An investigation of the azo-dye–doped LC systems following the approaches of our study, with emphasis on characterizing separately the dynamical responses of the various molecular species present after photoexcitation, could be readily carried out to answer the question whether the same physical mechanism, as elucidated in the present study, is at work in azo-dye–doped LC systems.

In terms of methodology, we would like to highlight that through judicious use of variable wavelengths and pulse sequences in the standard pump-probe technique, we have been able to characterize separately the dynamical responses of excited-state dye, ground-state dye, and host molecules, allowing us to directly follow the response of the host to the dye reorienting torque. This approach of looking at the host response is similar in spirit to recent studies of solvation dynamics in Refs. [30–32]. Our study, with picosecond excitation pulses, focuses exclusively on the diffusional reorientational dynamics, while the other studies, with femtosecond

excitation pulses, could probe the faster diffusion, libration, and interaction-induced responses [32]. The latter also found significant enhancement of the solvent responses upon electronic excitation of the guest molecules.

The success of the mean-field model in describing the guest-host interaction in isotropic dye-doped LC could yield insights into the nature of the LC host itself. Recall that in the isotropic phase the LC molecules still possess short-range orientational correlation, manifested as pseudonematic domains of finite size existing within the macroscopically isotropic material [36,37]. At the doping concentration that we used, it could be shown that we always have much less than one dye molecule per pseudonematic domains [73]. Thus, due to the short-range nature of the dipolar interaction responsible for the guest-host orientational coupling [35], the reorientation of LC by dye molecules is necessarily an intradomain process. The dye molecules are expected to couple to all modes of orientational relaxation [$k=1$ through 4 in Eq. (15)] of the LC host. While the $k=1$ component corresponds to collective response of LC following mean-field host-host coupling, components with $k \geqslant 2$ come from increasingly more local responses beyond the mean-field description of the host-host interaction [42]. More careful investigation of the reorientation enhancement by dye excitation in the short time regime could reveal how guest-host interaction affects reorientation of host molecules on different length scales [52,53].

An interesting prospect for future work is to search for the Jánossy effect in a pure LC medium, where the optical field electronically excites the host molecules themselves. If there is a substantial change in host-host interaction upon excitation, then enhanced molecular reorientation due to absorption may be realized, as has been theoretically proposed in Ref. [20]. Enhanced optical reorientation by excitation of host molecules, if significant, could provide a simple way of improving the nonlinearity of LCs for use in optoelectronics applications.

It would also be interesting to look for the Jánossy effect in chiral media. It is known that chiral dopants could induce or modify the chiral structure of nematic LCs through guest-host interaction [3,74]. A change in the chiral guest-host interaction by, for example, photoexcitation of the guest chiral molecules, would lead to a change in the macroscopic chirality of the system, as have been observed with chiral dopants that exhibits photoisomerization, providing new prospects for optoelectronic applications [75]. Photoexcited nonconformational chirality change of the chiral guest molecules could also induce a significant change in the chiral structure of the host. The chiral aminoanthraquinone dyes discussed in Ref. [76] seem particularly suited for a search for the chiral Jánossy effect.

This work was supported by U.S. National Science Foundation Grant No. DMR 9704384.

[1] I. C. Khoo and S. T. Wu, *Optics and Nonlinear Optics of Liquid Crystals* (World Scientific, New Jersey, 1993).
[2] B. Bahadur, in *Handbook of Liquid Crystals*, edited by D. Demus, J. Goodby, G. W. Gray, H-W. Spiess, and V. Vill (Wiley-VCH, New York, 1998), Vol. 2A.
[3] H-G. Kuball and T. Höfer, in *Chirality in Liquid Crystals*, edited by H-S. Kitzerow and C. Bahr (Springer, New York, 2001).
[4] T. Ikeda, J. Mater. Chem. **13**, 2037 (2003).
[5] L. Marrucci, Liq. Cryst. Today **11**, 1 (2002).
[6] L. Marrucci and Y. R. Shen, in *The Optics of Thermotropic Liquid Crystals*, edited by R. Sambles and S. Elston (Taylor & Francis, London, 1998).
[7] I. Jánossy, A. D. Lloyd, and B. S. Herrtt, Mol. Cryst. Liq. Cryst. **179**, 1 (1990).
[8] I. Jánossy and A. D. Lloyd, Mol. Cryst. Liq. Cryst. **203**, 77 (1991).
[9] I. Jánossy, L. Csillag, and A. D. Lloyd, Phys. Rev. A **44**, 8410 (1991).
[10] I. Jánossy and T. Kosa, Opt. Lett. **17**, 1183 (1992).
[11] K. Ichimura, Chem. Rev. (Washington, D.C.) **100**, 1847 (2000).
[12] I. C. Khoo, H. Li, and Y. Liang, IEEE J. Quantum Electron. **29**, 1444 (1993).
[13] D. Paparo, P. Maddalena, G. Abbate, E. Santamato, and I. Jánossy, Mol. Cryst. Liq. Cryst. Sci. Technol., Sect. A **251**, 73 (1994).
[14] T. Kosa and I. Jánossy, Opt. Lett. **20**, 1230 (1995).
[15] C. Manzo, D. Paparo, S. Lettieri, and L. Marrucci, Mol. Cryst. Liq. Cryst. **421**, 145 (2004).
[16] L. Marrucci, D. Paparo, P. Maddalena, E. Massera, E. Prudnikova, and E. Santamato, J. Chem. Phys. **107**, 9783 (1997).
[17] L. Marrucci, D. Paparo, M. R. Vetrano, M. Colicchio, E. Santamato, and G. Viscardi, J. Chem. Phys. **113**, 10362 (2000).
[18] M. Kreuzer, F. Hanisch, R. Eidenschink, D. Paparo, and L. Marrucci, Phys. Rev. Lett. **88**, 013902 (2002).
[19] D. Paparo, L. Marrucci, G. Abbate, E. Santamato, M. Kreuzer, P. Lehnert, and T. Vogeler, Phys. Rev. Lett. **78**, 38 (1997).
[20] L. Marrucci, D. Paparo, G. Abbate, E. Santamato, M. Kreuzer, P. Lehnert, and T. Vogeler, Phys. Rev. A **58**, 4926 (1998).
[21] R. Muenster, M. Jarasch, X. Zhuang, and Y. R. Shen, Phys. Rev. Lett. **78**, 42 (1997).
[22] I. Jánossy, Phys. Rev. E **49**, 2957 (1994).
[23] L. Marrucci and D. Paparo, Phys. Rev. E **56**, 1765 (1997).
[24] M. Kreuzer, L. Marrucci, and D. Paparo, J. Nonlinear Opt. Phys. Mater. **9**, 157 (2000).
[25] For a review see I. Jánossy, J. Nonlinear Opt. Phys. Mater. **8**, 361 (1999); and, in terms of a somewhat different picture, P. Palffy-Muhoray, T. Kosa, and E. Weinan, Appl. Phys. A **75**, 293 (2002).
[26] M. Kreuzer, E. Benkler, D. Paparo, G. Casillo, and L. Marrucci, Phys. Rev. E **68**, 011701 (2003).
[27] T. V. Truong, L. Xu, and Y. R. Shen, Phys. Rev. Lett. **90**, 193902 (2003); Phys. Rev. Lett. **93**, 039901(E) (2004).
[28] T. V. Truong and Y. R. Shen, J. Chem. Phys. **122**, 091104 (2005).
[29] For a review, see: R. M. Stratt and M. Maroncelli, J. Phys. Chem. **100**, 12981 (1996); G. R. Fleming and M. Cho, Annu.

Rev. Phys. Chem. **47**, 109 (1996); E. W. Castner and M. Maroncelli, J. Mol. Liq. **77**, 1 (1998); and references therein.
[30] D. F. Underwood and D. A. Blank, J. Phys. Chem. **107**, 956 (2003).
[31] S. J. Schmidtke, D. F. Underwood, and D. A. Blank, J. Am. Chem. Soc. **126**, 8620 (2004).
[32] S. Park, B. N. Flanders, X. Shang, R. A. Westervelt, J. Kim, and N. F. Scherer, J. Chem. Phys. **118**, 3917 (2003).
[33] Y. R. Shen, *The Principles of Nonlinear Optics* (John Wiley & Sons, New York, 1984).
[34] S. J. Clark in, *Physical Properties of Liquid Crystals: Nematics*, edited by D. A. Dunmur, A. Fukuda, and G. R. Luckhurst (INSPEC, London, 2001).
[35] J. N. Israelachvili, *Intermolecular and Surface Forces* (Academic Press, Inc., San Diego, 1987).
[36] P. G. de Gennes, Phys. Lett. **30A**, 454 (1969); Mol. Cryst. Liq. Cryst. **12**, 193 (1971).
[37] P. G. de Gennes, *The Physics of Liquid Crystals* (Clarendon Press, Oxford, UK, 1974).
[38] *Introduction to Liquid Crystals*, edited by E. B. Priestley, P. J. Wojtowicz, and P. Sheng (Plenum Press, New York, 1975).
[39] T. W. Stinson, III and J. D. Lister, Phys. Rev. Lett. **25**, 503 (1970).
[40] J. Prost and J. R. Lalanne, Phys. Rev. A **8**, 2090 (1973).
[41] G. K. L. Wong and Y. R. Shen, Phys. Rev. Lett. **30**, 895 (1973); Phys. Rev. A **10**, 1277 (1974).
[42] C. Flytzanis and Y. R. Shen, Phys. Rev. Lett. **33**, 14 (1974).
[43] N. M. Amer, Y. S. Lin, and Y. R. Shen, Solid State Commun. **16**, 1157 (1975).
[44] J. R. Lalanne, B. Martin, B. Pouligny, and S. Kielich, J. Opt. Commun. **19**, 440 (1976); Mol. Cryst. Liq. Cryst. **43**, 153 (1977).
[45] E. G. Hanson, Y. R. Shen, and G. K. L. Wong, Phys. Rev. A **14**, 1281 (1976).
[46] H. J. Coles, Mol. Cryst. Liq. Cryst. Lett. **49**, 67 (1978).
[47] B. Pouligny, E. Sein, and J. R. Lalanne, Phys. Rev. A **21**, 1528 (1980).
[48] F. W. Deeg, S. R. Greenfield, J. J. Stankus, V. J. Newell, and M. D. Fayer, J. Chem. Phys. **93**, 3503 (1990); J. J. Stankus, R. Torre, and M. D. Fayer, J. Phys. Chem. **97**, 9478 (1993).
[49] A. Sengupta and M. D. Fayer, J. Chem. Phys. **102**, 4193 (1994).
[50] R. Torre, M. Ricci, G. Saielli, P. Bartolini, and R. Righini, Mol. Cryst. Liq. Cryst. Sci. Technol., Sect. A **262**, 291 (1995); R. Torre and S. Califano, J. Chim. Phys. Phys.-Chim. Biol. **93**, 1843 (1996).
[51] S. Ravichandran, A. Perera, M. Moreau, and B. Bagchi, J. Chem. Phys. **109**, 7349 (1998).
[52] H. Cang, J. Li, V. N. Novikov, and M. D. Fayer, J. Chem. Phys. **119**, 10421 (2003).
[53] P. P. Jose and B. Bagchi, J. Chem. Phys. **120**, 11256 (2004).
[54] R. Zwanzig, J. Chem. Phys. **38**, 2766 (1963).
[55] H. Inoue, T. Hoshi, J. Yoshino, and Y. Tanizaki, Bull. Chem. Soc. Jpn. **45**, 1018 (1972).
[56] H. Inoue, M. Hida, N. Nakashima, and K. Yoshihara, J. Phys. Chem. **86**, 3184 (1982).
[57] R. W. Boyd, *Nonlinear Optics* (Academic Press, Inc., San Diego, 1992).
[58] M. A. Duguay and J. W. Hansen, Appl. Phys. Lett. **15**, 192 (1969).
[59] G. R. Fleming, J. M. Morris, and G. W. Robinson, Chem. Phys. **17**, 91 (1976).
[60] D. S. Alavi, R. S. Hartman, and D. H. Waldeck, J. Chem. Phys. **94**, 4509 (1991).
[61] N. Pfeffer, F. Charra, and J. M. Nunzi, Opt. Lett. **16**, 1987 (1991).
[62] See, e.g., I. Carmichael and G. L. Hug, Appl. Spectrosc. **41**, 1033 (1987); I. Carmichael, W. P. Helman, and G. L. Hug, J. Phys. Chem. Ref. Data **16**, 239 (1987).
[63] Our earlier work [28] reported different values for τ_f and τ_{Qe} compared to our present work. Reanalysis of the earlier data showed that we have underestimated the error. The correct result from that work should be $\tau_{Qe}=320\pm160$ ps (fluorescence experiment) and 360 ± 90 ps (dichroism experiment), and $\tau_f=1050\pm60$ ps. In light of the markedly better signal-to-noise ratio of the present result compared to the earlier results, we decided to use $\tau_{Qe}=490\pm30$ ps for further analysis of the guest-host interactions.
[64] D. Paparo, C. Manzo, and L. Marrucci, J. Chem. Phys. **117**, 2187 (2002).
[65] D. Reiser and A. Laubereau, J. Opt. Commun. **42**, 329 (1982); G. J. Blanchard and C. A. Cihal, J. Phys. Chem. **92**, 5950 (1988); G. J. Blanchard, J. Phys. Chem. **92**, 6303 (1988); D. S. Alavi, R. S. Hartman, and D. H. Waldeck, J. Chem. Phys. **95**, 6770 (1991); A. N. Rubinov and B. A. Bushuk, Laser Phys. **6**, 514 (1996); I. Ruckmann *et al.*, J. Opt. Commun. **170**, 361 (1999).
[66] G. Eyring and M. D. Fayer, J. Chem. Phys. **81**, 4314 (1984).
[67] H. J. Eichler, P. Günter, and D. W. Pohl, *Laser-Induced Dynamic Grating* (Springer-Verlag, Berlin, 1986).
[68] D. McMorrow, W. T. Lotshaw, and G. A. Kenney-Wallace, IEEE J. Quantum Electron. **24**, 443 (1988).
[69] P. P. Ho and R. R. Alfano, Phys. Rev. A **20**, 2170 (1979).
[70] R. J. W. Fèvre, A. Sundaram, and K. M. S. Sundaram, J. Chem. Soc., pp 974 (1963).
[71] The value of A/B here is different than what we stated in Ref. [28]. The latter was incorrect because we used wrong values for n and $\Delta\alpha_h'$.
[72] M. A. Osipov and E. M. Terentjev, Z. Naturforsch., A: Phys. Sci. **44**, 785 (1989).
[73] The size of pseudonematic domain is characterized by a correlation length ξ given by: $\xi=\xi_o[T^*/(T-T^*)]^{1/2}$ where ξ_o correponds to the LC molecular length. For 5CB, $\xi_o\simeq0.5$ nm and $T^*=34.2$ °C, so for $T=50$ °C and $T=T_{ni}=35.3$ °C, we have $\xi\simeq1.3$ and 8.8 nm, corresponding to domains containing $\simeq10$ and 500 LC molecules, respectively. The ratio of dye to LC molecules is $\simeq1:2000$.
[74] A. Ferrarini, G. J. Moro, and P. L. Nordio, Phys. Rev. E **53**, 681 (1996); M. A. Osipov and H. G. Kuball, Eur. Phys. J. E **5**, 589 (2001); G. Germano, M. P. Allen, and A. J. Masters, J. Chem. Phys. **116**, 9422 (2002); and reference therein.
[75] A. Yu. Bobrovsky, N. I. Boiko, V. P. Shibaev, and J. Springer, Adv. Mater. (Weinheim, Ger.) **12**, 1180 (2000); R. A. van Delden, M. B. van Gelder, N. P. M. Huck, and B. L. Feringa, Adv. Funct. Mater. **13**, 319 (2003).
[76] H. G. Kuball and H. Bruning, Chirality **9**, 407 (1997).